SCIENTIFIC REPORTS

OPEN

SUBJECT AREAS:
CONDENSED-MATTER PHYSICS
NANOSCALE MATERIALS
MAGNETIC PROPERTIES AND MATERIALS

Received
5 August 2013

Accepted
16 September 2013

Published
7 October 2013

Correspondence and requests for materials should be addressed to Z.H.C. (zhcheng@iphy.ac.cn)

Ultrafast demagnetization enhancement in CoFeB/MgO/CoFeB magnetic tunneling junction driven by spin tunneling current

Wei He, Tao Zhu, Xiang-Qun Zhang, Hai-Tao Yang & Zhao-Hua Cheng

State Key Laboratory of Magnetism and Beijing National Laboratory for Condensed Matter Physics, Institute of Physics, Chinese Academy of Sciences, Beijing 100190, China.

The laser-induced ultrafast demagnetization of CoFeB/MgO/CoFeB magnetic tunneling junction is exploited by time-resolved magneto-optical Kerr effect (TRMOKE) for both the parallel state (P state) and the antiparallel state (AP state) of the magnetizations between two magnetic layers. It was observed that the demagnetization time is shorter and the magnitude of demagnetization is larger in the AP state than those in the P state. These behaviors are attributed to the ultrafast spin transfer between two CoFeB layers via the tunneling of hot electrons through the MgO barrier. Our observation indicates that ultrafast demagnetization can be engineered by the hot electrons tunneling current. It opens the door to manipulate the ultrafast spin current in magnetic tunneling junctions.

The current trend in the spintronics devices with faster response demands the study of the magnetization dynamics of magnetic nanostructures on very small time scales[1]. In particular, laser induced demagnetization in ferromagnetic or ferrimagentic materials has attracted a growing interest, as it provides the ability to manipulate the magnetization using ultrashort optical pulses on subpicosecond timescale[2–6]. The understanding of the ultrafast demagnetization process is a very important issue not only for investigating the coupling between spin, electron and lattice in a strongly out-of-equilibrium regime, but also for potential application of spintronics devices working in terahertz regime[7]. Since the laser induced ultrafast demagnetization was first observed in Ni films[2], significant progresses have been made to explore the coupling between the laser excitation and the spin system[8–15]. The discussion of the coupling has been focused on the two exchange processes: energy exchange process and angular momentum exchange process. The whole process of energy exchange among the three thermal reservoirs: electron, phonon and spin, has been widely recognized by a phenomenological thermodynamic model, the so-called *three-temperature model*[3,8]. However, the intriguing exchange paths of angular momentum, especially, the dissipation channel of spin angular momentum, are still confused in the ultrafast demagnetization process. Mediated with photon[9], electron[10], phonon[11,12] and magnon[13], distinct spin-flip processes have been modeled as the dissipation channel of spin angular momentum for the loss of magnetization.

Most recently, the ultrafast spin transport of laser-excited hot electrons was considered as the dissipation channel of spin angular momentum to predict the ultrafast magnetization dynamics in magnetic layered- or hetero-structures[14,15]. After laser irradiation, the photo-excited electrons in metals that have been not cooled to the thermal equilibrium temperature are known as hot electrons. Transport of hot electrons in magnetic materials is spin dependent and has been modeled as *superdiffusive spin transport* to elucidate the influence of the transfer of spin angular momentum or spin current on the magnetization dynamics on few hundreds femtosecond timescale[15]. Recent experimental work has achieved significant progress for the predication of spin current and its considerable contribution to the ultrafast demagnetization. The giant ultrafast spin current was confirmed in Fe/Au and Fe/Ru heterostructures[7]. The demagnetization caused by superdiffusive spin current were observed not only in Fe/Au in which the hot electrons move from magnetic layer to non-magnetic layer[16], but also in Au/Ni in which the hot electrons move from non-magnetic layer to magnetic layer[17]. More interesting cases were reported on the time-resolved magnetization in magnetic metallic sandwiched structures Ni/Ru/Fe[18] and $[Co/Pt]_n/Ru/[Co/Pt]_n$[19]. The superdiffusive spin current in Ni/Ru/Fe magnetic multilayers results in an enhancement in the magnetization of bottom Fe layer within several picoseconds when the magnetic configuration of two layers

is parallel[18]. The demagnetization in multilayer $[Co/Pt]_n$ is enhanced by the spin current when the magnetic configuration for the $[Co/Pt]_n$/layers is antiparallel[19]. Hence the ultrafast spin transport has a considerable contribution in the ultrafast demagnetization.

The superdiffusive spin current opens a door to engineer the spin transfer in magnetic sandwiched structures in terahertz regime. However, the space layer between two magnetic layers must be spin transmitter and most of choice was a thin metal Ru film[18,19]. It was pointed out that the superdiffusive spin current will be weaker by a metal film Ta or W, and will be blocked by an insulating layer NiO or Si_3N_4[19,20]. Although the magnetic tunneling current has been identified in magnetic multilayer sandwiched by a thin insulator Al_2O_3 or MgO layer[21,22], the ultrafast spin transport in magnetic tunneling junctions was not reported yet. Here, we present a laser induced ultrafast demagnetization in sandwiched CoFeB films with an insulating MgO film as the space layer. In contrast to insulating NiO space layer, where the ultrafast demagnetization processes same between P and AP states are same[19], it was observed in CoFeB/MgO/CoFeB magnetic tunneling junction that the demagnetization time becomes shorter and the magnitude of demagnetization becomes larger when the magnetic configuration was varied from P state to AP one. This finding can be explained by the transfer of spin angular momentum via the tunneling spin current in two magnetic layers. Our observations indicate the ultrafast spin current can tunnel through the insulating MgO layer and control the speed and efficiency of ultrafast demagnetization.

Results

Fig. 1 shows the static polar hysteresis loop of CoFeB/MgO/CoFeB multilayered film (see the Methods section). The square loop indicates the film has perpendicular magnetic anisotropy (PMA). The hysteresis loop shows two distinct switching fields separated by a large antiferromagnetic plateau and is constituted by two minor loops, for top and bottom CoFeB layers respectively. The minor loop of with lower switching field is counted and plotted in Fig. 1. According to the loops in fig. 1, the magnetic directions of the two CoFeB layers can be controlled by external magnetic field. When the applied reversal field is in between the two switching fields, their magnetization directions are antiparallel (AP state). However, when the applied field is large enough to overcome the higher switching field, the magnetizations of both FeCoB layers are aligned in the same direction (P state). The magnetization directions for both CoFeB multilayers are depicted in Fig. 1 for different magnetic applied fields.

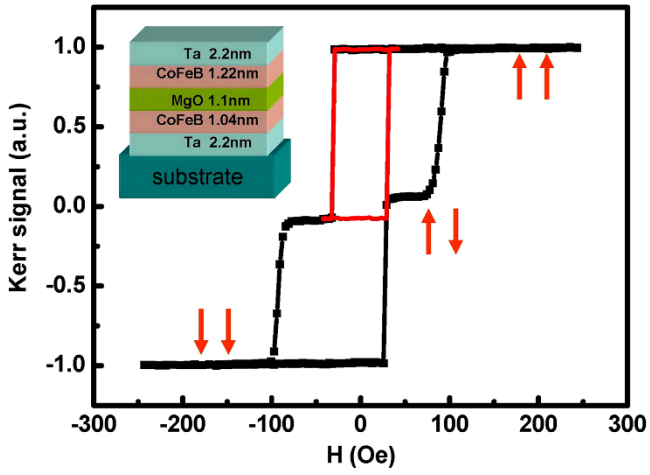

Figure 1 | The normalized Kerr loop for CoFeB/MgO/CoFeB film. The black curve is the major loop and the red curve is the minor loop with lower switching field. The pair of arrows presents the magnetization configuration. The inset is the structure of the sample.

The two distinct switching fields suggest that the two CoFeB layers have different perpendicular magnetic anisotropy fields. The magnetizations characterized by polarized neutron reflectometry are 663 emu/cm^3 and 906 emu/cm^3 for top layer and bottom layer, respectively[23]. The bottom layer with the high magnetization has a small PMA and the small switching field is $H_1 = 29$ Oe, while the top layer with the low magnetization has a large PMA and the large switching field is $H_2 = 84$ Oe. For the AP state, the normalized magnetization is 8%, which is in good agreement with the result of polarized neutron reflectometry (7.6%). This consistence infers that the optical depth-dependent profile can be neglected due to the thickness of CoFeB/MgO/CoFeB film is less than the optical penetration depth.

Figure 2(a) depicts the dynamic signals of ultrafast demagnetization under the pump fluence 2.94 mJ/cm^2 for the P and AP states (see the Methods section). When the pump laser heats the sample, a decrease in the magnitude of the magnetization is observed in time less than 400 fs. Then, a subsequent recovery is occurred within a few ps. Owing to the large PMA to suppress the reorientation of the magnetization, no signature of the magnetic precession was observed for the time delay up to 1 ns in both P and AP states (not shown here). Since the reorientation of the magnetization is absent, the dynamic change of the Kerr signal presents the amplitude of the magnetization loss. We write the magnetization loss as $-\Delta M_{z,i} = \lambda_i^s M_{z,i}$, where λ_i^s is defined as the coefficient of magnetization loss ($i = 1,2$ for top and bottom layers, and $s =$ P, AP state, respectively). The measured magnetization losses $-\Delta M_z$ are $-\Delta M_z^{AP} = \lambda_2^{AP} M_{z,2} - \lambda_1^{AP} M_{z,1}$ and $-\Delta M_z^P = \lambda_2^P M_{z,2} + \lambda_1^P M_{z,1}$ for the AP and P states,

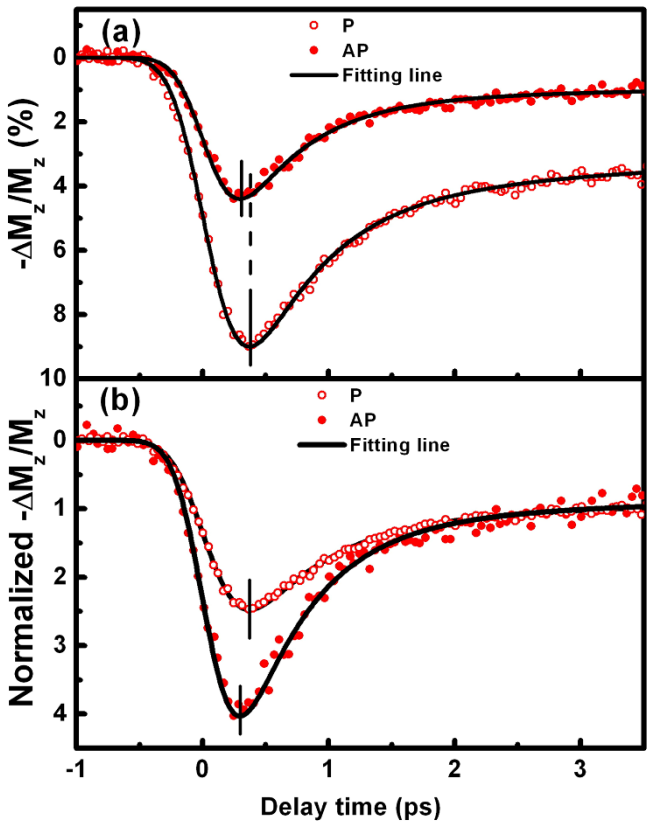

Figure 2 | TRMOKE measured ultrafast magnetization dynamical signal in CoFeB/MgO/CoFeB film at parallel and antiparallel states. (a) Measures signal. (b) Normalized curves of TRMOKE signals (normalized at 2 ps). Full and empty circular dots present the parallel state (P) and antiparallel state (AP), respectively. The solid lines are fits to the experimental data.

respectively. Compared the demagnetization curves in the P and AP states, the times for demagnetization reached the maximum are different (line indicated in Fig. 2(a)) and the demagnetization time was accelerated in the AP state. The maximum values of measured magnetization loss $-\Delta M_z^{AP}$ and $-\Delta M_z^{P}$ are 4.4% and 8.9% of the saturated magnetization $M_z = M_{z,1} + M_{z,2}$ for AP and P states, respectively.

To obtain more quantitative understanding of the femtosecond laser induced demagnetization dynamics in CoFeB/MgO/CoFeB film, the experimental data were fitted with a function based on the three-temperature model[8,19]:

$$-\frac{\Delta M_z}{M_z} = \left\{ \left[\frac{A_1}{(t/\tau_0+1)^{0.5}} - \frac{(A_2\tau_E - A_1\tau_M)}{\tau_E - \tau_M} e^{-\frac{t}{\tau_M}} - \right. \right. \\ \left. \left. - \frac{\tau_E(A_1 - A_2)}{\tau_E - \tau_M} e^{-\frac{t}{\tau_E}} \right] \Theta(t) + A_3\delta(t) \right\} * G(t) \quad (1)$$

where *G(t) presents the convolution product with the Gaussian laser pulse profile, Θ(t) is the step function, $\delta(t)$ is the Dirac delta function, and A_i (I = 1,2,3) are the constants. The two time parameters τ_E and τ_M describe the dynamical process of demagnetization. τ_E characterizes the relaxation time of electron-phonon interaction that energy equilibrates the electron with the lattice. τ_M characterizes the demagnetization time when energy deposited into the spin system. The fitting curve is plotted in Fig. 2 (a). The value of $\tau_E = 570 \pm 30$ fs is the best fitting value for both P and AP states. The electron-phonon relaxation time is in good agreement with previous measurements on other ferromagnetic metals films[19]. Interestingly, the value of τ_M depends on the magnetic configuration: 90 ± 5 fs for AP state and 120 ± 5 fs for the P state. Hence the demagnetization process in AP state is 25% faster than in the P state.

The curves in Fig. 2(a) are normalized at 3 ps and the normalized curves in the P and AP states are plotted in Fig. 2(b). In order to compare the normalized magnetization loss induced by femtosecond laser excitation for the AP state with that for the P state, the ratio of magnetization loss in the AP to P states is defined as $R = (\lambda_2^{AP} M_{z,2} - \lambda_1^{AP} M_{z,1})/(\lambda_2^{P} M_{z,2} + \lambda_1^{P} M_{z,1})$. For t > 3 ps, the three reservoirs reach the thermal equilibrium and the coefficient of magnetization loss λ_i^s only depends on the heating temperature[24]. The thermal equilibrium temperatures are dominated by the lattice reservoir and are same for the P and AP states. So $\lambda_i^P = \lambda_i^{AP}$ for each layer when t > 3 ps and get $\lambda_2 \approx 1.58\lambda_1$ with R = 0.3. The difference of coefficient of magnetization loss means that the two magnetic layers have different temperature-dependent magnetization profiles. As seen in fig. 2 (b), the amount of the demagnetization increases about ~ 65% in the AP state compared with the P state.

The maximum amplitudes of demagnetization in the P and AP states were measured with various pump fluences for gaining more physical insight into the enhanced demagnetization in the AP state. Two parameters were counted: maximum of magnetization loss in the P and AP states. Figure 3 (a) shows the magnetization losses as a function of the pump fluence. When the pump fluence is increased from 0.29 to 3.92 mJ/cm², the demagnetization for the P state increases linearly from 0.9% to 11.6%. The linear relationship is broken when the fluence is increased up to 4.9 mJ/cm², while the demagnetization reaches 12.0%. If there is no magnetic correlation between the two separated CoFeB layers, the sample can be considered as two individual magnetic layers and λ_i^P Equals λ_i^{AP}. In this case, $\lambda_2 \approx 1.58\lambda_1$ is assumed and $-\Delta M_z^{AP,n} = \lambda_2^P M_{z,2} - \lambda_1^P M_{z,1}$, which present the measured demagnetization in the AP state without magnetic correlation, is evaluated for the fluence below 3.92 mJ/cm². The evaluated values in the AP state for magnetic correlation are indicated as well as the experimental data $-\Delta M_z^{AP}$ in Fig. 3(a). The experimental data is close to evaluated value at 0.29 mJ/cm² but larger than evaluated one when pump fluence is above 0.49 mJ/cm².

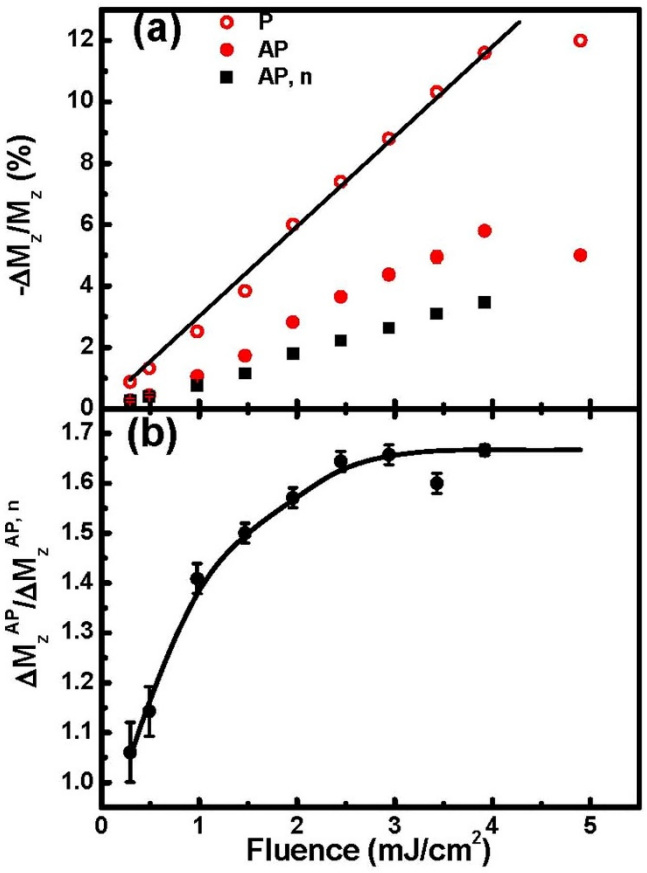

Figure 3 | (a) The magnetization loss and (b) the enhancement magnetization loss at AP state as the function of the pump fluence. Full circular dots, empty circular dots present the magnetization loss at parallel state (P), antiparalle state (AP), respectively. Full square dots present the evaluated AP values without magnetic correlation between two magnetic layers (see the text). The solid lines are guided to the experimental data.

The larger experimental values reveal that the demagnetization is enhanced in the AP state compared to the P state. In order to stress the enhancement related to magnetic correlation, $\Delta M_z^{AP}/\Delta M_z^{AP,n}$ is plotted in Fig. 3(b). An increasing relation between the enhancement and the pump fluence is visible in Fig. 3(b) when the fluence is lower than 2.45 mJ/cm². $\Delta M_z^{AP}/\Delta M_z^{AP,n}$ approximately keeps at a constant 1.66 when fluence is in range of 2.45 to 3.92 mJ/cm². The enhancement for 4.9 mJ/cm² is not calculated since the laser irradiation is stronger than the low fluence limit. The data in Fig. 3(b) indicates that the magnetic correlation enhances the ultrafast magnetization in CoFeB/MgO/CoFeB film in the AP state.

Discussion

In the frame of three temperature model, the energy transfers from electrons to spin system and thereby an increase of the spin temperature is launched. This laser heat effect causes the demagnetization through the local spin-flip scattering as the dissipation channel of spin angular momentum[9–13]. However, the thermalized process for the hot electrons is not included in the three temperature model[15]. This process launches the ultrafast spin transport in ferromagnetic materials and the nonlocal transfer of spin angular momentum[17–19]. In spite of the contribution of spin flip scattering on the ultrafast demagnetization process, the ultrafast spin transport was emphasized to explain the faster demagnetization time and enhancement of magnetization loss in the AP state[18–20]. To assess this point, we demonstrate the role of the ultrafast spin transport in CoFeB/MgO/

CoFeB film. When CoFeB and Ta layers absorb pump laser, hot electrons are generated. In magnetic materials, spin-majority and spin-minority hot electrons have distinctly transport properties due to their different lifetimes and velocities. Compared with spin-majority electrons, spin-minority electrons have shorter lifetime and diffusion length. Therefore, the spin-minority electrons is more easily and faster trapped in the local exciting region (electrons generated by magnetic layers themselves) or at interface (electrons coming from adjacent layers)[15]. Consequently this transient accumulation of spin-minority hot electrons in CoFeB film layer results in the demagnetization. For each individual magnetic layer of sandwiched CoFeB/MgO/CoFeB film, the hot electrons consist of three sources: spin-polarized electrons generated by themselves, non-polarized electrons coming from capping or buffer layer, and additionally spin-polarized electrons transferring from other magnetic layer. Here, we focus on the transport of hot electrons causes the transfer of spin angular momentum between two individual magnetic layers. Nevertheless the MgO film is an insulating layer, the hot electrons can not diffuse through it but can tunnel through it[25,26]. Furthermore, the MgO barrier is a spin filter and filters out all tunneling states other than the Δ_1 band and the Δ_1 band of CoFeB only consists of spin-majority electrons[5,21,27].

Once the hot spin-majority electrons of top (bottom) magnetic layer tunnel to bottom (top) layer, the spin current has distinct functions for demagnetization in the P and AP states. For simplifying the discussion, the tunneling current J_1 and J_2 are defined as from top to bottom layer and from bottom to top layer. The function of spin tunneling current is demonstrated in Fig. 4. In the P state, the net spin current J_1–J_2 is zero for the assumption of local charge neutrality. If we count the population between spin-majority and spin-minority, change is not happen by tunneling current in Fig. 4(a). The spin transfer of tunneling current in the P state has little influence for the demagnetization of sandwiched CoFeB film. Conversely in the AP state, the spin-majority electrons will become spin-minority electrons when they tunnel into other magnetic layer. Both top and bottom layers lose the spin-majority electrons and receive the spin-minority electrons. As seen in Fig. 4 (b), the difference of population between spin-majority and spin-minority is reduced by the net spin current $J_1 + J_2$ and enhance the demagnetization for both two CoFeB layers. As a result, the ultrafast spin tunneling current adds a dissipation path for spin angular momentum to accelerate the demagnetization time for CoFeB/MgO/CoFeB film in the AP state.

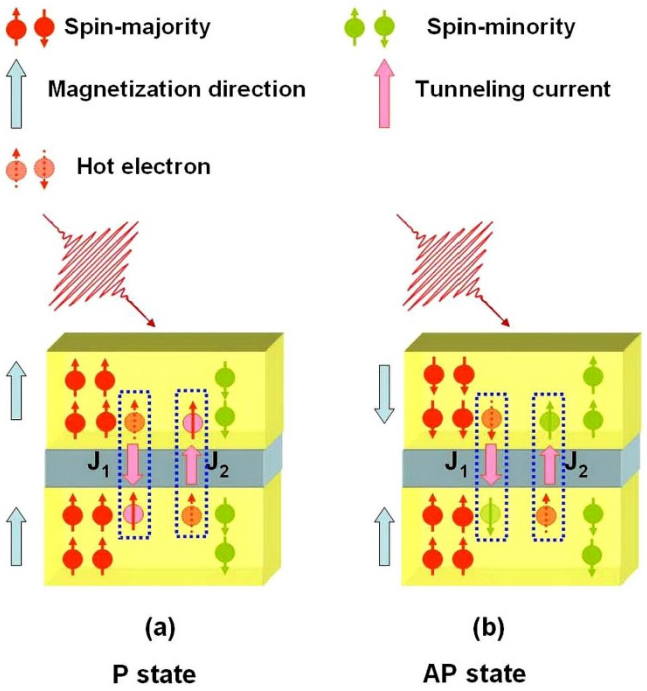

Figure 4 | Schematic diagrams of hot tunneling spin current in CoFeB/MgO/CoFeB film after laser excitation. (a) Diagram for parallel state and (b) for antiparallel state.

Even the spin tunneling current $J_1 + J_2$ enhance the demagnetization for both two CoFeB layers in the AP state, the measured magnetization loss $-\Delta M_z{}^{AP}$ ($= \lambda_2^{AP} M_{z,2} - \lambda_1^{AP} M_{z,1}$) will not change since the enhanced demagnetizations by tunneling current have been canceled for measurement. In order to explain the enhanced $-\Delta M_z^{AP}$, other mechanisms of ultrafast demagnetization are concluded. Now the dissipation channels of spin angular momentum in CoFeB/MgO/CoFeB film principally include spin-flip scattering[11], superdiffusive spin current[14] and spin tunneling current. The coefficient of magnetization loss λ is formally written as

$$\lambda = \lambda_{spin-flip} + \lambda_{superdiffusive} + \lambda_{tunneling}. \quad (2)$$

The $\lambda_{spin\text{-}flip}$, $\lambda_{superdiffusive}$ and $\lambda_{tunneling}$ are defined as the characteristic coefficients of the magnetization loss caused by spin-flip scattering, superdiffusive spin current and spin tunneling current, respectively. The $\lambda_{spin\text{-}flip}$ and $\lambda_{superdiffusive}$ dependent on the population of spin-majority and spin minority. The spin tunneling currents change the population of spin-majority and spin minority for each CoFeB layers in the AP state and then influence the $\lambda_{spin\text{-}flip}$ and $\lambda_{superdiffusive}$. This influence causes the variations of the $\lambda_{spin\text{-}flip}$ and $\lambda_{superdiffusive}$ for each CoFeB layers. The variation is different for top and bottom magnetic layer and the enhancements of total demagnetization loss for the two magnetic layers are different in the AP state. The data in Fig. 3(b) indicates the enhancement of the demagnetization in bottom CoFeB layer is larger than that in top layer. The first increase and then saturation of enhancement along with increasing laser fluence infers the intriguing competitive relationship among the different demagnetization mechanisms. A compatible model includes the spin transport (superdiffusive spin current and tunneling spin current) and spin-flip scattering is required to explore the ultrafast demagnetization in magnetic nanostructures[28].

Finally, the ultrafast spin tunneling current in CoFeB/MgO/CoFeB sandwiched film transfers the spin angular momentum between two magnetic layers and controls the ultrafast demagnetization. Our observation indicates that ultrafast demagnetization can be engineered by the hot tunneling current. This finding may open a new route to manipulate the spin transport in magnetic tunneling junctions within few hundred femtoseconds.

Methods

Sample description. The stack structure of CoFeB(1.22 nm)/MgO(1.1 nm)/CoFeB(1.04 nm) were deposited by magnetron sputtering with a base pressure of 4×10^{-6} Pa. The numbers in brackets are nominal thickness. A thin 2.2 nm Ta seed layer was first deposited on thermally oxidized silicon substrates. Another thin 2.2 nm Ta layer covered CoFeB/MgO/CoFeB film to protect against oxidation. The stack structure of the sample is present in the insert of Fig. 1. The sample was then annealed at 300°C in a vacuum chamber for an hour. Argon was used as the sputtering gas. The sputtering pressure for metals was 0.4 Pa and for MgO layers was 0.2 Pa. High purity $Co_{40}Fe_{40}B_{20}$ (99.9%), MgO (99.99%), and tantalum (99.95%; all obtained from Functional Materials International, Japan) were used as the target materials.

Experimental method. The static polar Kerr loop of CoFeB/MgO/CoFeB film was acquired using a laser diode with a wavelength of 650 nm. The dynamical process of ultrafast demagnetization was measured by TRMOKE. The experiments were carried out using an all optical pump-probe technique. A train of optical pulse with 780 nm wavelength, 55 fs duration and 100 nJ/pulse is generated at 5.2 MHz repetition rate by a Ti:sapphire oscillator (FEMTOLASER, XL-100). We doubled the frequency of the femtosecond laser via a nonlinear optical crystal BaB_2O_4 (BBO) with a thickness of 200 μm. The laser beam is split into a 780 nm laser beam and a 390 nm laser beam by a dichroic beamsplitter. The 780 nm laser is used as pump pulse to excite the magnetic system out of equilibrium, while the 390 nm laser is much weaker than that of the 780 nm beam (1 : 100) and is used as probe pulse to measure the subsequent magnetization dynamical response with timescale from subpicosecond to nanosecond. The time resolved measurement is realized by varying the time delay between pump and probe pulse. In this experiment the pump beam was focused down

to the sample 10 μm spot by a 20 × objective at normal incidence. The used detection geometry is sensitive to the out-of-plane component of the magnetization M_z. The pumping laser induced change of the Kerr signal presents the change of the magnetization $\triangle M_z$. The pump fluence is in the range of 0.29 to 4.9 mJ/cm^2 and the external field was applied perpendicular to the film plane. Before the TRMOKE measurement, the CoFeB/MgO/CoFeB film was saturated at −120 Oe. Then the experimental data were acquired at 50 Oe (AP state) and 120 Oe (P state), respectively.

1. Hillebrands, B. & Ounadjela, K. *Topics of Applied Physics: Spin Dynamics in Confined Magnetic Structures II* (Springer, New York, 2003).
2. Beaurepaire, E. *et al.* Ultrafast spin dynamics in ferromagnetic Nickel. *Phys. Rev. Lett.* **76**, 4250 (1996).
3. Kirilyuk, A., Kimel, A. & Rasing, Th. Ultrafast optical manipulation of magnetic order. *Rev. Mod. Phys.* **82**, 2731 (2010).
4. Boeglin, C. *et al.* Distinguishing the ultrafast dynamics of spin and orbital moments in solids. *Nature* **465**, 458–462 (2010).
5. Mann, A. *et al.* Insights into ultrafast demagnetization in pseudogap half-metals. *Phys. Rev. X* **2**, 041008 (2012).
6. Graves, C. E. *et al.* Nanoscale spin reversal by non-local angular momentum transfer following ultrafast laser excitation in ferrimagnetic GdFeCo. *Nature Mater.* **12**, 293 (2013).
7. Kampfrath, T. *et al.* Teraherz spin current pulses controlled by magnetic heterostructures. *Nature Nanotech.* **8**, 256–260 (2013).
8. Axitia, U. *et al.* Evidence for thermal mechanisms in laser induced femtosecond spin dynamics. *Phys. Rev. B* **81**, 174401 (2010).
9. Vonesch, H. *et al.* Ultrafast spin-photon interaction investigated with coherent magneto-optics. *Phys. Rev. B* **85**, 180407 (2012).
10. Krauβ, K. *et al.* Ultrafast demagnetization of ferromagnetic transition metals: The role of the Coulomb interaction. *Phys. Rev. B* **80**, 180407 (2009).
11. Cinchetti, M. *et al.* Spin-flip processes and ultrafast magnetization dynamics in Co: unifying the microscopic and macroscopic view of femtosecond magnetism. *Phys. Rev. Lett.* **97**, 177201 (2006).
12. Carva, K. *et al. Ab* initio theory of electron-phonon mediated ultrafast spin relaxation of laser-excited hot electrons in transition-metal ferromagnets. *Phys. Rev. B* **87**, 184425 (2013).
13. Carpene, E. *et al.* Dynamics of electron-magnon interaction and ultrafast demagnetization in thin iron films. *Phys. Rev. B* **79**, 174422 (2008).
14. Battiato, M. *et al.* Superdiffusive spin transport as a mechanism of ultrafast demagnetization. *Phys. Rev. Lett* **105**, 027203 (2010).
15. Battiato, M. *et al.* Theory of laser-induced ultrafast superdiffusive spin transport in layered heterostructures. *Phys. Rev. B* **86**, 024404 (2012).
16. Melnikov, A. *et al.* Ultrafast transport of laser excited spin polarized carriers in Au/Fe/MgO(001). *Phys. Rev. Lett.* **107**, 076601 (2011).
17. Eschenlohr, A. *et al.* Ultrafast spin transport as key to femtosecond demagnetization. *Nature Mater.* **12**, 332 (2013).
18. Rudolf, D. *et al.* Ultrafast magnetization enhencement in metallic multilayers driven by superdiffusive spin current. *Nat. Commun.* **3**, 1037 (2012).
19. Malinowski, G. *et al.* Control of speed and efficiency of ultrafast demagnetization by direct transfer spin angular momentum. *Nature Phys.* **4**, 855 (2008).
20. Turgut, E. *et al.* Controlling the competition between optically induced ultrafast spin-flip scattering and spin transport in magnetic multilayers. *Phys. Rev. Lett.* **110**, 197201 (2013).
21. Butler, W. H. *et al.* Spin-dependent tunneling conductance of Fe/MgO/Fe sandwiches. *Phys. Rev. B* **63**, 054416 (2001).
22. Ando, Y. *et al.* Spin-dependent tunneling spectroscopy in single-crystal Fe/MgO/Fe tunneling junctions. *Appl. Phys. Lett.* **87**, 142502 (2005).
23. Zhu, T. *et al.* The study of perpendicular magnetic anisotropy in CoFeB sandwiched by MgO and tantalum layers using polarized neutron reflectometry. *Appl. Phys. Lett.* **100**, 202406 (2012).
24. Koopmans, B. *et al.* Ultrafast Magneto-Optics in Nickel: Magnetism or Optics? *Phys. Rev. Lett* **85**, 844 (2000).
25. van Dijken, S., Jiang, X. & Parkin, S. P. Non monotonic bias voltage dependence of the magnet current in GaAs-Based magnetic tunnel transistors. *Phys. Rev. Lett.* **90**, 197203 (2003).
26. Le Breton, J. C. *et al.* Thermal spin current from a ferromagnet to silicon by Seebeck spin tunneling. *Nature* **475**, 82–85 (2011).
27. Yuasa, S. & Djayaprawira, D. D. Giant tunnel magnetoresistance in magnetic tunnel junctions with a crystalline MgO(001) barrier. *J. Phys. D: Appl. Phys.* **40**, R337 (2007).
28. Schellekens, A. J. & Koopmans, B. Comparing ultrafast demagnetization rates between competing models for finite temperature magnetism. *Phys. Rev. Lett.* **110**, 217204 (2013).

Acknowledgements

This work was supported by the National Basic Research Program of China (973 program, Grant Nos. 2012CB933102, 2010CB934202, and 2011CB921801) and the National Natural Sciences Foundation of China (51201179, 11274361, 11034004, 50931006). We thank Prof. J.W. Cai for his careful reading and constructive suggestions for the manuscript.

Author contributions

W.H. and Z.H.C. conceived the experiments. T.Z. fabricated the sample. W.H. carried out the experiments. X.Q.Z. and H.T.Y. have some contributions for the TRMOKE setup. All the co-authors contributed to the analysis and discussion for the results. W.H. and Z.H.C. wrote the paper and all the co-authors comment on it.

Additional information

Competing financial interests: The authors declare no competing financial interests.

How to cite this article: He, W., Zhu, T., Zhang, X., Yang, H. & Cheng, Z. Ultrafast demagnetization enhancement in CoFeB/MgO/CoFeB magnetic tunneling junction driven by spin tunneling current. *Sci. Rep.* **3**, 2883; DOI:10.1038/srep02883 (2013).